Electronic Supplementary Material (ESI) for Journal of Materials Chemistry A.

Supporting Information

Exploring AIE Luminogens as stickers to construct self-healing ionomers and as probes to detect the microscopic healing dynamics

Shiyu Gu, Hao Wang, Hao Zhang, Yan Peng, Linjun Zhang, Junqi Zhang, Jing Zheng and Jinrong Wu*

State Key Laboratory of Polymer Materials Engineering, College of Polymer Science and Engineering, Sichuan University, Chengdu 610065, China.

***Corresponding author:** E-mail: wujinrong@scu.edu.cn

1 Experimental Section

1.1 Raw Materials

All commercially available materials, reagents and solvents were used as supplied, unless otherwise stated including Potassium Carbonate (Greagent, >99.0%), Silica gel (Greagent, 300-400 mesh), Tetrabutylammonium Bromide (TBAB, Adamas, 99.0%), Tetrakis(triphenylphosphine)palladium (Pd $(PPh_3)_4$, Adamas, 9.2%(Pd)), Ethyl Acetate (EA, Greagent, ≥99.7%), Hexane (Greagent, ≥97.0%), Tetrahydrofuran (THF, Greagent, ≥99.5%), Triethylamine (Adamas, 99.0%), Pyridine-4-Boronic Acid (PyPba, Adamas, 98.0%), Anhydrous dichloromethane (DCM, Adamas,99.0%), Tetraphenylethylene (TPE, TCI, 98.0%),Acryloyl Chloride(AC, Adamas, >98.0%), Bromotriphenylethylene (P_3Br, TCI, 98.0%), methyl methacrylate (MMA, Adamas, 99.0%), 2,2-Azobis(isobutyronitrile) (AIBN, TCI, 98.0%), Trimethylene Bromohydrin (Adamas, >98.0%). N-butyl acrylate (nBA, TCI, 99.0%) was filtered through a plug of basic alumina oxide before use, Ethyl Acetate for synthesis (EA, Adamas, 99.8%), THF for synthesis was distilled from Na/benzophenone prior to use. Triphenyl vinylpyridines (PyTPE) and 1-bromo-butylacrylate (VBr) were synthesized referring to literatures (Scheme S1a and S1b).

1.2 Sample preparation

The three-necked flask was evacuated under vacuum and flushed with argon for three times before reaction starting. All reactions were carried out under a dry argon atmosphere and the temperatures were measured externally.

1.2.1 Synthesis of 1-bromo-butylacrylate (VBr).

Procedures for the synthesis of VBr were shown in Scheme S1a. In a 250 mL three-necked flask, trimethylene Bromohydrin (25 g, 0.1799 mol), 100ml anhydrous DCM and triethylamine (21.8411 g, 1.2 eqv) were added. Cooling down to 0 ℃ and slowly added acrylyl chloride dissolved in 30 ml anhydrous DCM (19.5360 g, 1.2 eqv), then stirred for 1 h. The reaction was then warmed to room temperature and stirred for 24 h. After that, 450 ml deionized water and 150 ml saturated salt water were used to wash organic phase, and the excess solvent was removed by rotary evaporator. The product

was brown liquid and obtained in 76% yield. The chemical structure of VBr was confirmed by solution ^{1}H NMR spectroscopy shown in Fig. S1. ^{1}H NMR (400 MHz, $CDCl_3$) δ 6.39 (1 H, d, J 17.3), 6.10 (1 H, dd, J 17.3, 10.4), 5.83 (1 H, dd, J 10.4, 1.3), 4.29 (2 H, dd, J 11.5, 5.5), 3.54 (2 H, dt, J 60.1, 6.5), 2.17 (2 H, m).

1.2.2 Synthesis of triphenyl vinylpyridines (PyTPE).

Procedures for the synthesis of PyTPE were shown in Scheme S1b through the convenient Suzuki coupling reaction[1]. In a 250 ml three-necked flask, P_3Br (2.00 g, 5.97 mmol), PyPba (0.8801 g, 7.16 mmol) and 50ml THF were added and stirred uniformly. Then, 12 ml 2 M K_2CO_3 and TBAB (0.16g) were added and stirred at R.T. for 0.5 h. After that, Pd $(PPh_3)_4$ (0.3 g) was added and heated flask to 85 ℃ for 24 h. After cooling to R.T., the mixture was added to deionized water (50 ml) and extracted with DCM until the extract became colorless. The collected organic layer was dried with anhydrous Na_2SO_4. After the solvent have been evaporated under reduced pressure, the crude product was purified by a silica gel column using hexane/ ethyl acetate (10:1, v: v) as eluent to give PyTPE as a yellow solid with 89% yield. The chemical structure of PyTPE was confirmed by solution ^{1}H NMR spectroscopy and FTIR as shown in Fig. S2. ^{1}H NMR (400 MHz, $CDCl_3$) δ 8.26 (d, J = 6.1 Hz, 1H), 7.11 (dd, J = 9.4, 4.7 Hz, 1H), 7.05 (ddd, J = 10.9, 9.8, 3.2 Hz, 4H), 6.98 – 6.92 (m, 3H), 6.92 (d, J = 4.9 Hz, 1H).

1.2.3 Synthesis of poly (BA-MMA-VBr) (PBMB).

PBMB was synthesized by one-pot free-radical copolymerization at 80 ℃ for 10 h using butyl acrylate (BA), methyl methacrylate (MMA) and 1-bromo-butylacrylate (VBr) at 60:40:3 molar ratio (Tab. S1). After that, the crude product was precipitated in n-hexane and dissolved in THF, repeated 3 times at R.T to obtain a solid, then dried in a vacuum oven at 40 ℃ for 48 h. Br-free contrast sample poly (BA-MMA) (PBM) was synthesized by the same way. The chemical structure of PBMB was confirmed by solution ^{1}H NMR spectroscopy, FTIR and GPC as shown in Fig. S3 and Tab. S1, respectively.

1.2.4 Synthesis of PBMB-PyTPE.

Fabrication of PBMB-PyTPE by alkylation reaction with PBMB (1.0133 g) and PyTPE

(1 eq, 0.0828 g). The mixture was slowly poured into PTFE mold, then maintained at R.T and 40 °C in vacuum oven for 24 h respectively to remove the solvent. After that, it was reacted at 140 °C for 40 min as Scheme S2 shown. The chemical structure of PBMB-PyTPE was confirmed by ^{1}H NMR spectroscopy and FTIR as shown in Fig. S4.

2 Methods and techniques

2.1 Fourier transform infrared spectroscopy (FTIR)

FTIR spectra were recorded using Thermo Scientific Nicolet iS50 FTIR by an attenuated total reflection (ATR) mode at room temperature. The on-line tracing of ionic bonds is conducted through the transmission mode at room temperature. The wavenumber scale was from 4000 cm^{-1} to 400 cm^{-1}.

2.2 Nuclear Magnetic Resonance (NMR)

The ^{1}H NMR spectra were measured on a Bruker AV III HD spectrometer operating at 400 MHz in $CDCl_3$ (δ (^{1}H) = 7.26 ppm) or DMSO (δ (^{1}H) = 2.5 ppm) with TMS as reference.

2.3 Differential scanning calorimeter (DSC)

The heat flow curves of elastomers were acquired on the Q2000 (TA instruments). The sample was firstly heated from 25 ℃ to 100 ℃ and then cooled from 100 ℃ to -70 ℃ with the rate of 20 ℃/min to eliminate thermal history, and then the sample was heated from -70 ℃ to 100 ℃ with the rate of 10 ℃/min to record the heat flow. The glass transition temperature (T_g) of the samples were defined as the inflection point of the heating curves.

2.4 Dynamic mechanical analysis (DMA)

Dynamic mechanical properties were measured on the Q800 (TA instruments) in the tension mode. The geometry rectangular samples with the sizes about 10 mm (length) *5 mm (width) *0.3 mm (thickness) were heated from -70 ℃ to 100 ℃ with the heating rate of 5 ℃/min, the frequency of 1 Hz and the preload force of 0.01 N.

2.5 Gel permeation chromatography (GPC)

The molecular weight and polydispersity index (PDI) of the PBMB were measured by

GPC at room temperature (Tosoh HIC-8320GPC, THF as the eluent and PMMA as the standard).

2.6 Rheology

The rheological measurements were carried out by the HAAKE MARS (Mars III). Frequency sweeping from 0.01 Hz to 100 Hz was conducted at range of 283 K-413 K, the temperature gradient and strain was 10 K and 1%, respectively. Master curves, were obtained by shifting the frequency sweeping curves at different temperatures to 283 K. The samples were the disks with diameter 20 mm and thickness 0.5 mm and the tests were performed in torsion mode. In all the dynamic shear experiments, the strain deformation was fixed at 0.1%, which was small enough to avoid the nonlinear response (Fig. S7b) and large enough to have a reasonable signal intensity. Oscillatory frequency sweep tests were performed in the range of 0.1-100 rad s^{-1} with 0.1% strain.

2.7 Atomic force microscope (AFM)

AFM height diagrams were gotten by AIST-NT SPM smartSPMTM-1000 in the tapping (AC) mode with the spring constant of 70 N/m and the resonance frequency of 289 kHz. Sample preparation: PBMB-PyTPE was dissolved in THF with the concentration of 0.1 mg/ml. Spin coated the solution on the silicon slice using the spin coater (KW-4A). Afterwards the silicon slice was placed in the vacuum oven at 100 ℃ for 30 mins.

2.8 Tensile test

Tensile experiments were performed on an Instron 5967 tensile tester. Samples were cut into the dumbbell shape by a normalized cutter with the gauge length of 15 mm, the width of 2 mm and the thickness of 0.3-0.6 mm. For the samples of mechanical healing test, the crack with 50-100 μm was produced by blade. Uniaxial tensile measurements were performed at room temperature in the air with the strain rate of 100 mm/min. The Young's modulus was determined by the slope within the initial linear region of the stress-strain curves.

2.9 Small-angle X-ray scattering (SAXS)

SAXS experiments were performed at room temperature at the BL16B1 beamline of the Shanghai Synchrotron Radiation Facility (SSRF). The wavelength of the X-rays

used was 0.124 nm. Two-dimensional SAXS patterns were recorded with a MAR-CCD detector (MAR, USA). The image acquisition time for each frame was 1 s. The distance from sample to detector in SAXS experiments was 2000 mm. The SAXS patterns were background corrected and processed using Fit2D software for further analysis.

2.10 Confocal laser scanning microscope (CLSM)

CLSM images were taken by Zeiss LSM 700 with 5× and 10× objective. The excitation wavelength was 405 nm, and the emission wavelength was received at a range of 495-630 nm. A fresh scratch was created on the surface of PBMB-PyTPE film, and the photos of the scratch healing process was taken every 0.5 h for a total of 4 h. All images of this experiment were captured under the same conditions in terms of objective amplification (x10), gain limit (600), and ambient temperature (25 ℃). The images of three-dimensional curves were acquired through the MATLAB (software version: R2018a) mesh function.

2.11 Fluorescence spectra

The fluorescence spectra were recorded with a Horiba FluoroMax-4 spectrometer at the excitation wavelength of 365 nm under room temperature, unless otherwise stated. As we know, the film-forming conditions (i.e., film-forming methods, solution properties and apparatus) have an impact on the fluorescence intensity through affecting the packing density of molecular chains, chain conformation and molecular mobility. For a substrate supported film, simulations had revealed that near a confining interface the conformations of polymer chains were highly perturbed[2]. Therefore, in order to make experiments more scientific and minimize the effect of film forming conditions on fluorescence tests, we used the same method for solution-casting film (Scheme S2), film thickness was maintained at 0.3mm-0.6mm, and only the change of fluorescence intensity on the free surface of a same membrane with external fields was studied.

Gradient stretching fluorescence was carried out by spectral acquisition mode, basic parameter including: integration time: 0.1 s, increment: 1.00 nm, dark offset. The experimental procedure was as follows: stretched 10s (total 60 s) waiting a full spectrum (40 s)，then recovered 10 s (total 40 s) waiting a full spectrum (40 s). **Stress relaxation fluorescence** was carried out by kinetics mode, basic parameter including:

integration time: 0.1 s, interval time: 0.10 s, increment: 1.00 nm, dark offset. The experimental procedure was as follows (used 30 mm/min as an example): stretched 60 s with tensile rate 30 mm/min waiting a full spectrum (40 s), then unloaded stress but kept the strain constant, switched mode and set signal emission wavelengths (selected the peak of the full spectrum). **Variable temperature fluorescence** was carried out by spectral acquisition mode, and temperature control accessories was added, basic parameter same as gradient stretching fluorescence. **Crack healing fluorescence** was carried out spectral acquisition mode, and excited light acted on scratch, basic parameter same as gradient stretching fluorescence.

3 THEORY AND CALCULATION

3.1 Self-healing efficiency

General healing efficiency (η) is calculated according to the following equation:

$$\eta = \frac{\sigma_{heal}}{\sigma_{original}} \times 100\%$$

Where σ_{heal} is the tensile strength of the healing samples, and $\sigma_{original}$ is the tensile strength for the original samples.

Self-healing efficiency η_{PLM} calculated by crack width through Adobe Illustrator (software version: Ai2021) as Fig. S5 shown and the result shown in Tab. S2:

$$\eta_{PLM} = \frac{W_{crack} - W_{heal}}{W_{crack}} \times 100\%$$

Where W_{heal} is the crack width of the healing samples, and W_{crack} is the crack width for the initial scratched samples.

Self-healing efficiency η_{CSLM} calculated by fluorescence intensity read by MATLAB data cursor tool as Fig. S6 shown and the result shown in Tab. S3:

$$\eta_{CSLM} = \frac{I_{heal} - I_{crack}}{I_{original}} \times 100\%$$

Where I_{heal} is the fluorescence intensity of the healing samples, I_{crack} and $I_{original}$ is the fluorescence intensity before and after the scratch.

Self-healing efficiency η_{FL} calculated by relative fluorescence intensity characterized by fluorescence spectra directly:

$$\eta_{FL} = \frac{I_{heal} - I_{crack}}{I_{original}} \times 100\%$$

Where I_{heal} is the fluorescence intensity of the healing samples, I_{crack} and $I_{original}$ is the fluorescence intensity before and after the scratch.

3.2 Activation energy

The activation free energy barrier relates to the lifetime of a sticker τ_s, in the simplest form, through the Arrhenius equation:

$$\tau_s = \tau_0 \exp\left(\frac{E_a}{RT}\right)$$

Where E_a is the activation energy, R is Avogadro constant and τ_0 is proportionality constant.

3.3 Noda's rule for the generalized 2D correlation spectra[3]

If the correlation intensity Φ (v1, v2) in synchronous spectra has the same symbol (positive or negative) as the correlation peak Ψ (v1, v2) in asynchronous spectra, then the movement of band v1 is prior to or earlier than that of band v2, and vice versa. Besides, if the correlation intensity in synchronous spectra is not zero (or blank), but zero in asynchronous one, then the movements of bands at v1 and v2 are simultaneous. Noda's rules are summarized as follows:

(1) If Φ (v1, v2) > 0, Ψ (v1, v2) > 0 or Φ (v1, v2) < 0, Ψ (v1, v2) < 0, then the movement of v1 is before than that of v2.

(2) If Φ (v1, v2) > 0, Ψ (v1, v2) < 0 or Φ (v1, v2) < 0, Ψ (v1, v2) > 0, then the movement of v1 is after than that of v2.

(3) If Φ (v1, v2) > 0, Ψ (v1, v2) = 0 or Φ (v1, v2) < 0, Ψ (v1, v2) = 0, then the movements of v1 and v2 are simultaneous.

Φ (v1, v2) and Ψ (v1, v2) represent the correlation peaks in synchronous and asynchronous spectra, respectively.

FIGURES AND TABLES

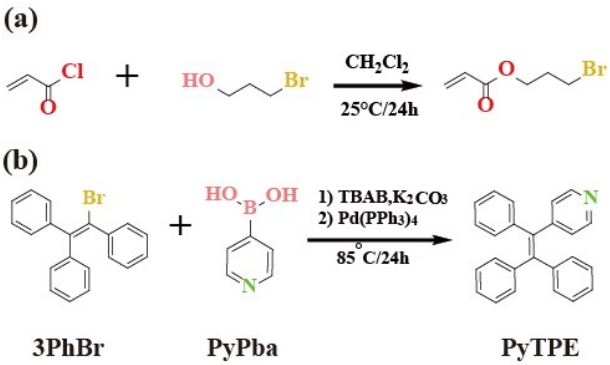

Scheme S1. Synthetic procedures of monomers.

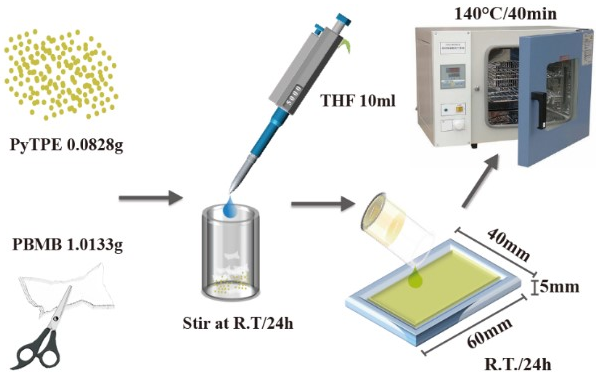

Scheme S2. Preparation of PBMB-PyTPE by casting film.

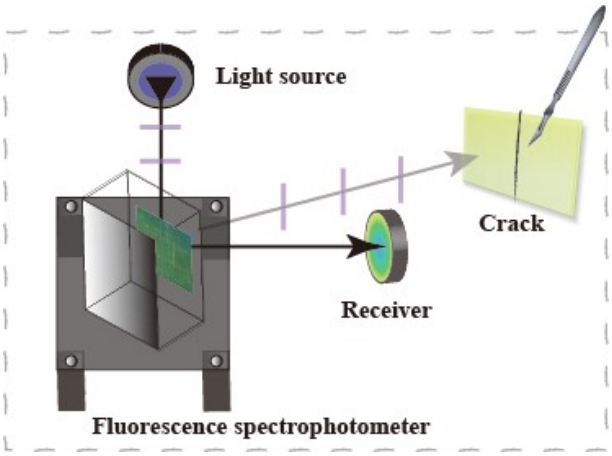

Scheme S3. Illustration of healing fluorescence test.

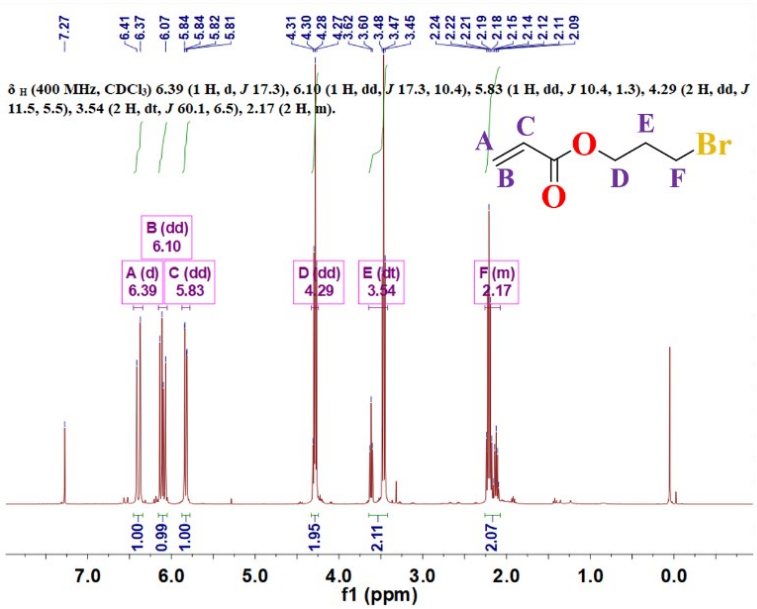

Figure S1. [1]HNMR Spectra of VBr. The solvent was $CDCl_3$ (δ ([1]H) = 7.26 ppm).

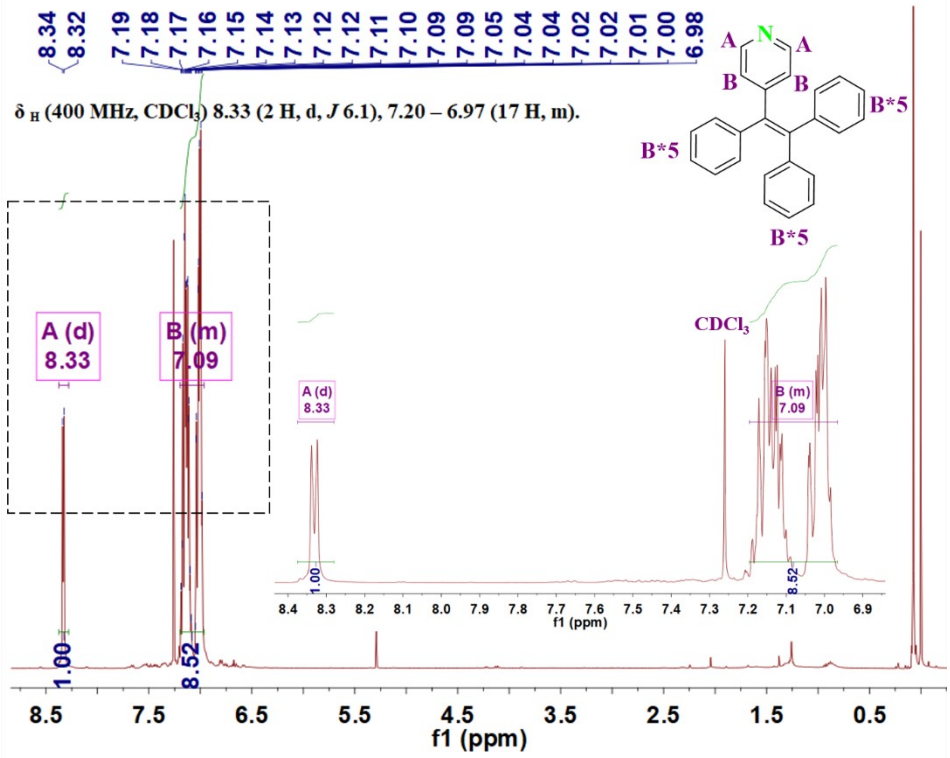

Figure S2. [1]HNMR Spectra of PyTPE and and the inserted graph is a magnification of the dotted part. The solvent was $CDCl_3$ (δ ([1]H) = 7.26 ppm).

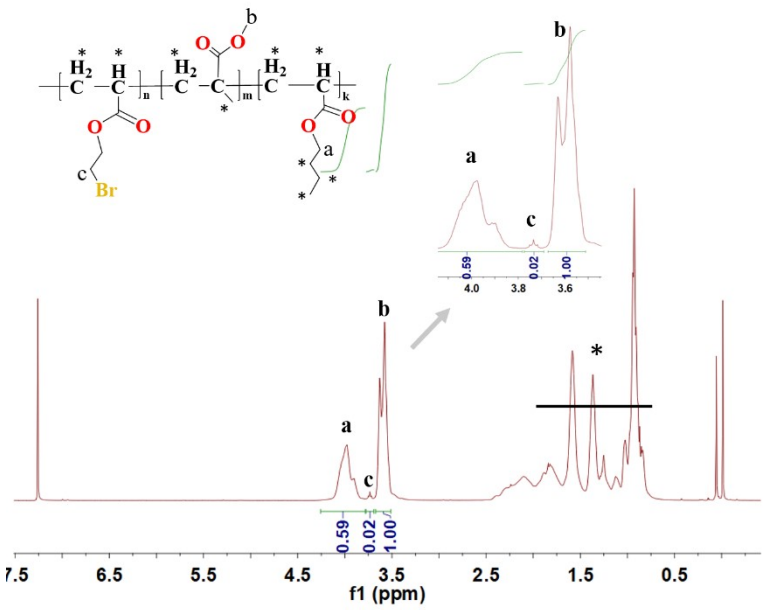

Figure S3. ^{1}HNMR Spectra of PBMB. The solvent was $CDCl_3$ (δ (^{1}H) = 7.26 ppm).

Comments: Copolymer compositions were determined by measuring the resonance intensities of nBA-OCH_2–,MMA –OCH_3 and VBr-$BrCH_2$- at 4.03,3.62 and 3.73 ppm based on Fig. S3, respectively[4]. Actual molar ratio (nBA : nMMA : nVBr) = $\frac{\int 4.03ppm/2}{\sum\left(\int 4.03ppm/2 + \int 3.62ppm/2 + \int 3.73ppm/2\right)}$: $\frac{\int 3.62ppm/3}{\sum\left(\int 4.03ppm/2 + \int 3.62ppm/2 + \int 3.73ppm/2\right)}$: $\frac{\int 3.73ppm/2}{\sum\left(\int 4.03ppm/2 + \int 3.62ppm/2 + \int 3.73ppm/2\right)}$ = 46 : 52 : 1.57

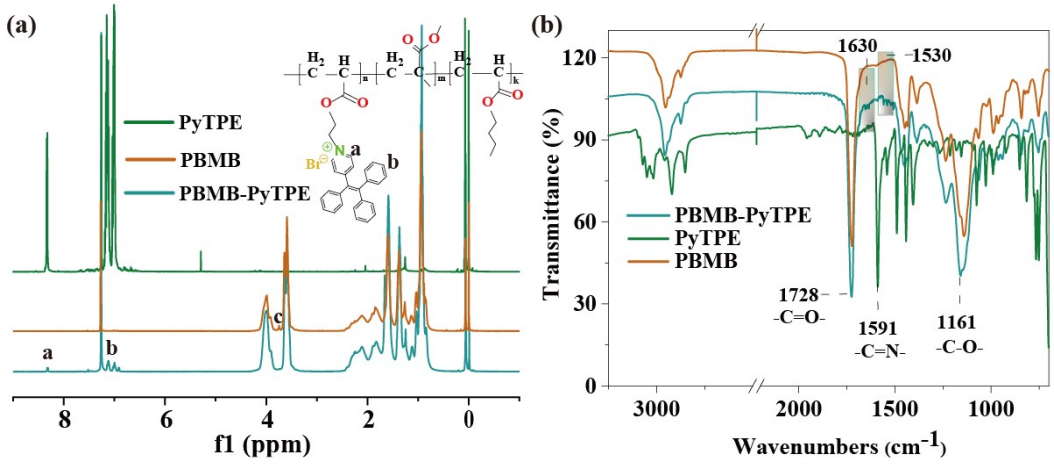

Figure S4. ^{1}H NMR (a) and FTIR (b) Spectra of PBMB-PyTPE and compared with PBMB and

PyTPE. The solvent was $CDCl_3$ (δ (^1H) = 7.26 ppm).

Comments: The characteristic peaks of PyTPE ring at a and b appeared and the peak at c of -C$^1H_2$-Br disappeared in PBMB-PyTPE. The bending vibrations of -C=O and -C-O-C at 1728 cm^{-1} and 1161 cm^{-1} corresponding to the presentation of acrylate units remains unchanged due to their nonreactivity. The peak at 1590 cm^{-1} disappeared nearly which belonged to the bending vibrations of -C=N on the pyridine ring[5], and new peaks shown at 1630 cm^{-1} and 1530 cm^{-1} were attributed to the ionic interation between pyridine and bromo[6]. The results of ^{1}HNMR and FTIR investigated that the successful synthesis of PBMB-PyTPE through the alkylation reaction between the bromine atoms and pyridyl groups.

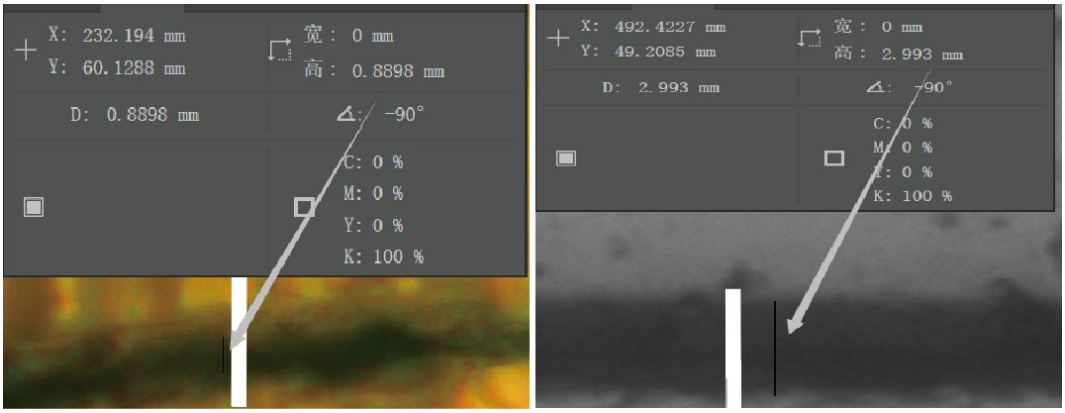

Figure S5. Self-healing efficiency calculated by AI: crack healing efficiency η_{PLM} calculated by crack width measured by AI measurement tool（Three-point average）.

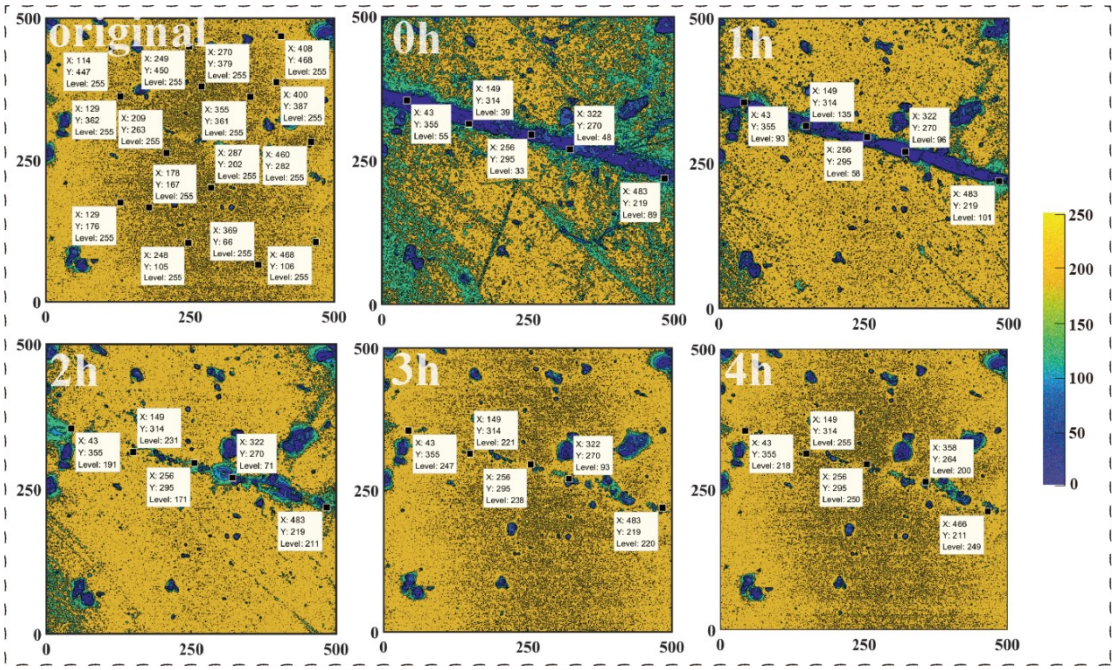

Figure S6. Self-healing efficiency calculated by MATLAB (software version: R2018a): Crack healing efficiency η_{CLSM} calculated by fluorescence intensity read by MATLAB data cursor tool（Five-points average）.

Comments: From Fig. S6, decreased fluorescence also presented around the crack due to activated

adjacent moieties. Then the fluorescence intensity enhanced rapidly as thermodynamically stable structures were generated within each fragment of the broken material, indicating that dangling chains containing a high concentration of dissociated bonds following initial fracture tended to diffuse back into the bulk polymer.

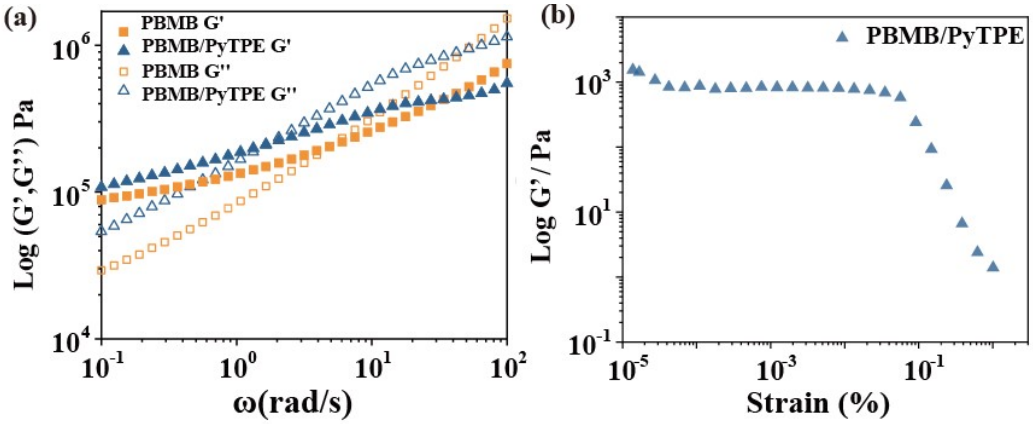

Figure S7. Rheology properties of PBMB-PyTPE: (a) Oscillatory frequency sweep test (R.T.); (b) Linear viscoelastic region.

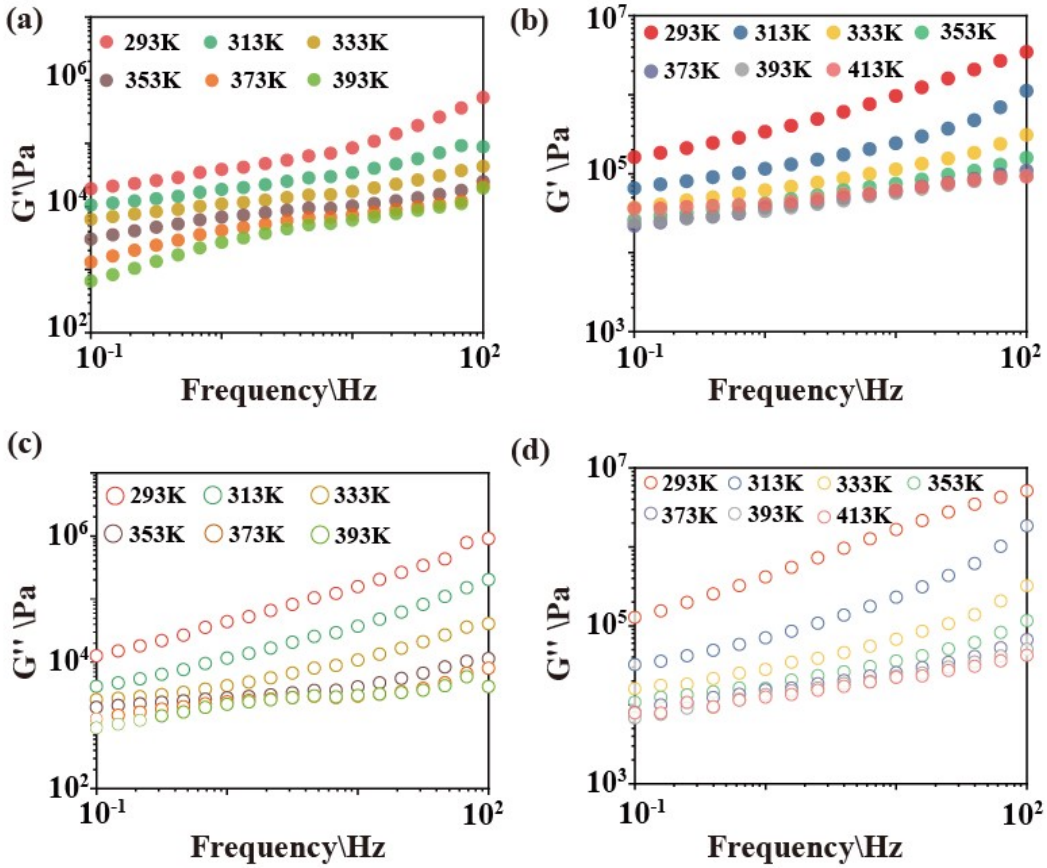

Figure S8. Graphs of frequency sweeping before TTS shift: G' of (a)contrast sample PBMB and (b) PBMB-PyTPE; G'' of (c) contrast sample PBMB and (d) PBMB-PyTPE.

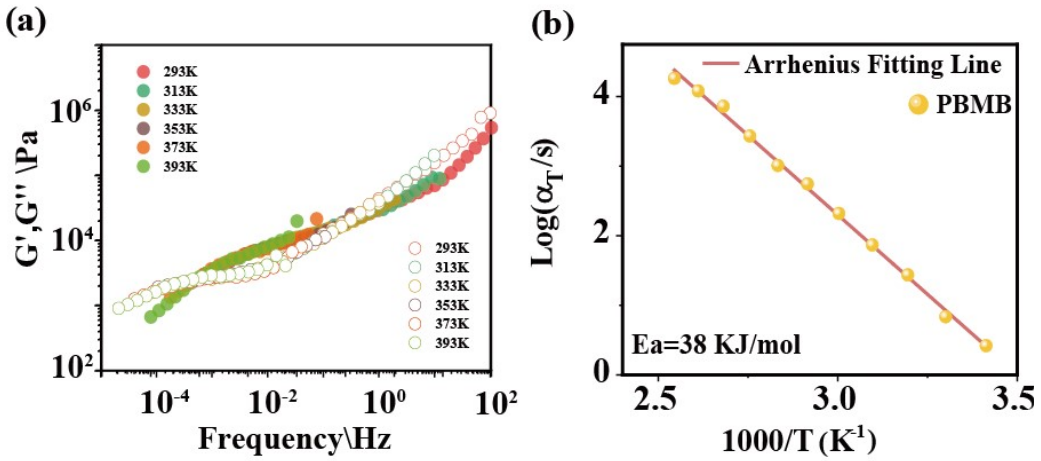

Figure S9. Viscoelastic properties of contrast sample PBMB. (a) Master curve: lg G' and lg G'' as a function of the logarithm of frequency (lg f), T_{ref}= 283 K, T_{max}=393 K; (b) Shift factors that fitted using the Arrhenius equation.

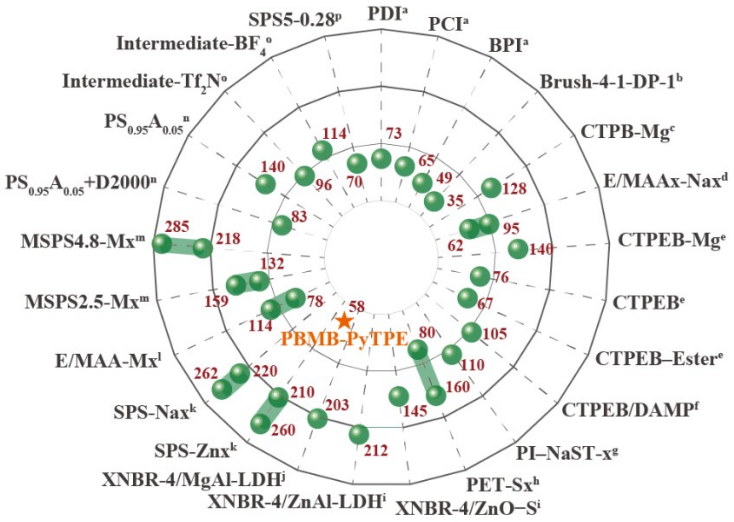

Figure S10. Activation Energies (Ea, KJ/mol) of PBMB-PyTPE compared for other reported ionic polymers. a) Bromobutyl rubber (BIIR) with different pyridine-based derivatives[7]; b) Bottle-brush ionomer based on terminal bromide-pyridine bonds[8]; c) Telechelic polybutadiene-magnesium ionomer[9]; d) E/MAA Copolymers with different Na wt%[10]; e) Mg neutralized telechelic poly(ethylene butylene) ionomer[11]; f) Carboxyl terminated poly(ethylene butylene) (CTPEB) composited with 1,5-diamino-2-methyl pentane (DAMP)[12]; g) Poly(ethylene–acrylic acid) neutralized by zinc salts[13]; h) Afullyneutralized sulfonatemoiety (sodiosulfo) isophthalate (SIP) modified with polyethylene terephthalate) (PET)[14]; i) Carboxylated nitrile rubber (XNBR) with ZnO−S and zinc−aluminum-based layered double hydroxide (ZnAl-LDH)[15]; j) Lightly sulfonated polystyrene ionomers[16]; k) Ethylenemethacrylic acid (E/MAA) ionomers neutralized with various cation[17]; l) Oligomeric sulfonated polystyrene MSPS[18]; m) Diamineneutralized entangled poly(styrene-co-4-vinylbenzoic acid) ionomers[19]; n) Imidazolium-based ionomers with different counterions and side chain lengths[20]; o) Ethylene-methacrylic acid (E/MAA) ionomers with different MAA wt% and neutralization with Na salt[21]; p) sulfonated polystyrene (SPS) with different sulfonation levels[22].

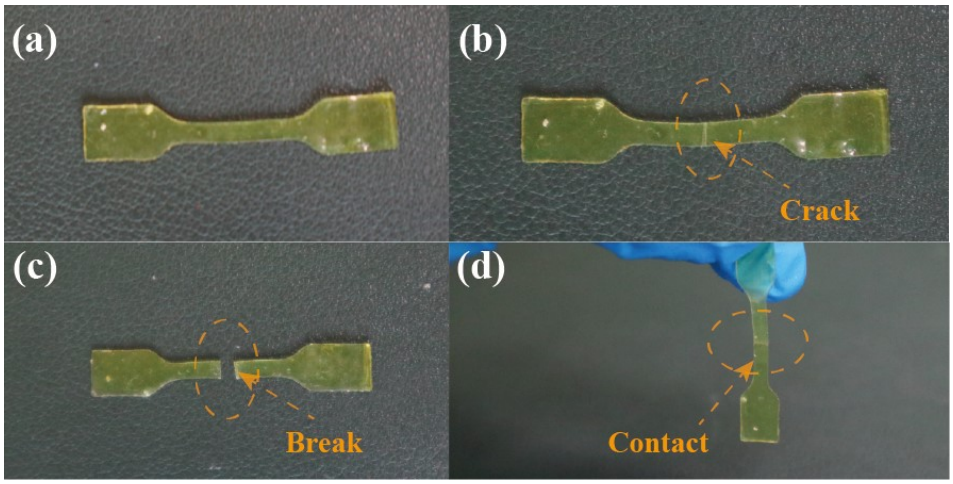

Figure S11. Illustration of the difference between crack and break. (a) Untreated sample; (b) Cracked sample; (c) Broken sample; (d) Contact the broken sample.

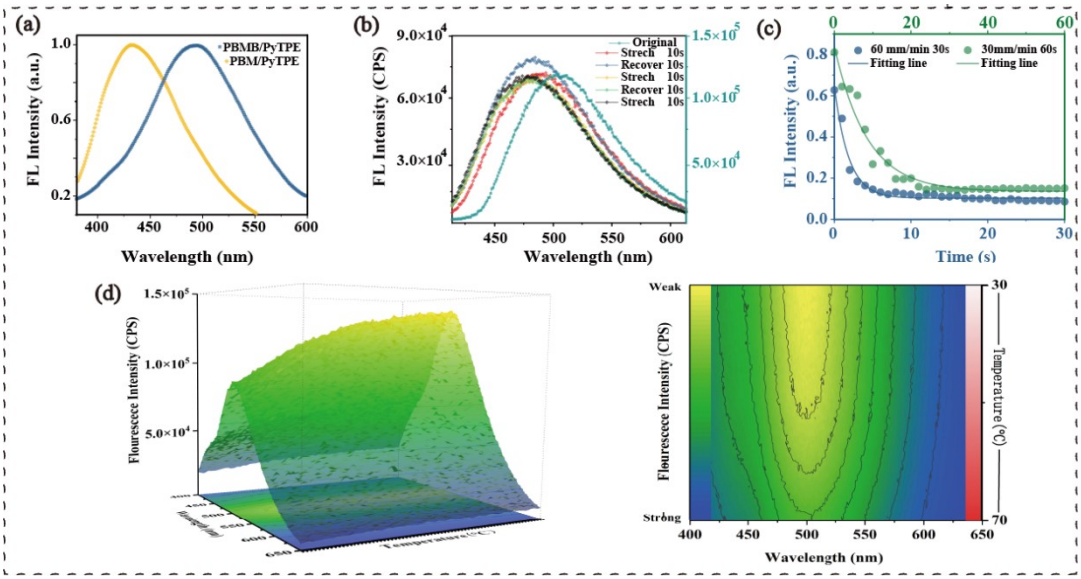

Figure S12. Fluorescence property of PBMB-PyTPE ((λ_{ex}=365 nm). (a) Fluorescence spectra of PBMB-PyTPE and bromine-free PBM-PyTPE, a transform of excitation wavelength from blue luminescence to yellow fluorescence; (b) Fluorescence spectra of PBMB-PyTPE after fully stretching-recovering cycle; (c) Dynamic fluorescence intensity change of PBMB-PyTPE at tensile rate of 60 mm/min and 30 mm/min, exponential fitting function: $y=31804e^{-0.017x}$ and $y=24858e^{-0.004x}$, respectively; (d) Cooling fluorescence spectra of PBMB-PyTPE from 70 °C to 30 °C.

Comments: The AIE effect of PyTPE had been confirmed by Pigge et al[23],while the formation of sticky groups would produce an AIEE effect, showing an obvious red shift of the emission peak in Fig. S12a[24]. For the gradient stretching fluorescence test, the stretching process is also a film thickness changing process.

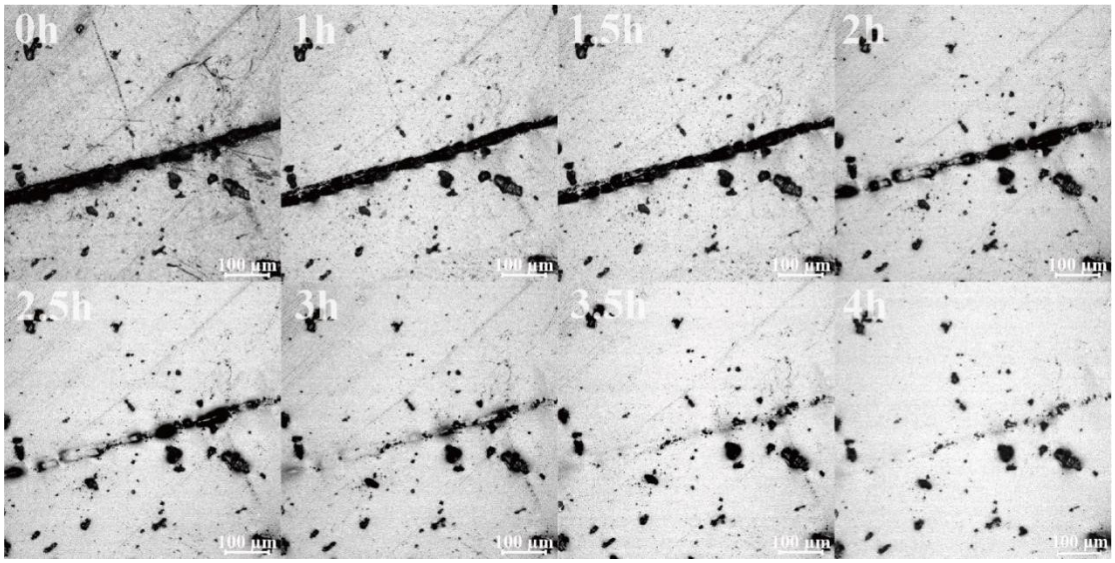

Figure S13. Photos of crack carried out by CLSM from 0 h to 4 h under R.T (Scale bar: 100 μm).

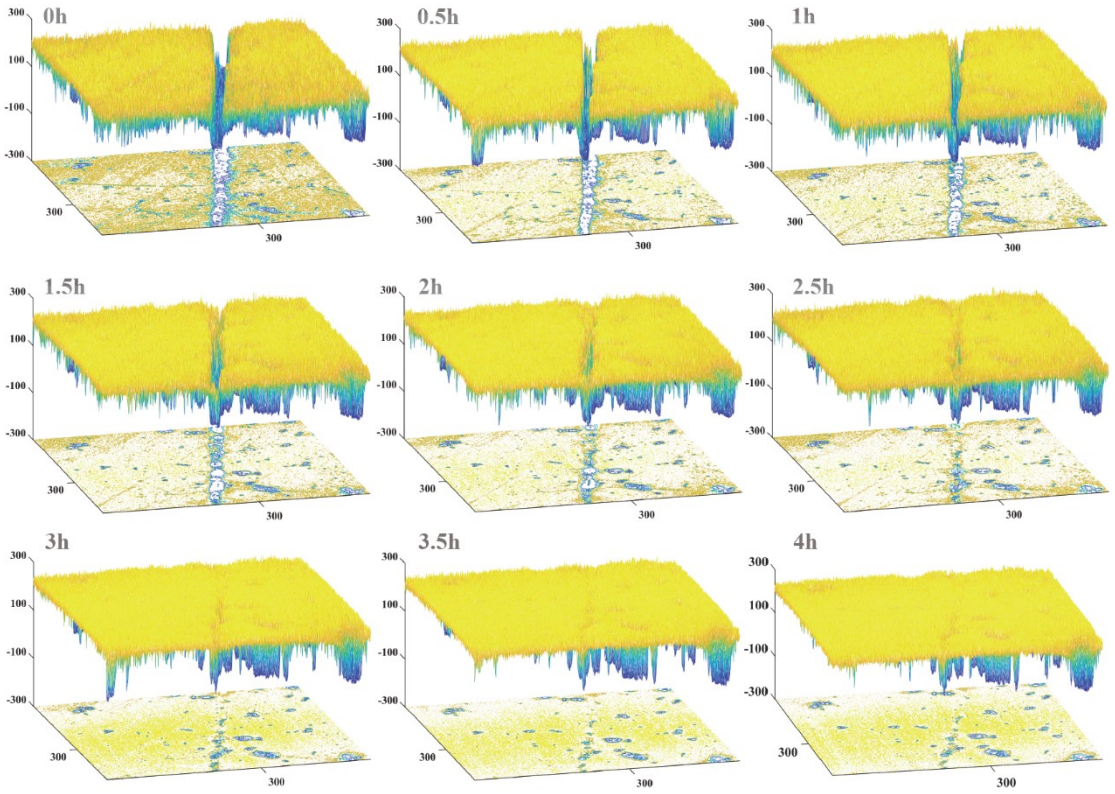

Figure S14. CLSM photos of crack from 0 h to 4 h at R.T and processed by MATLAB.

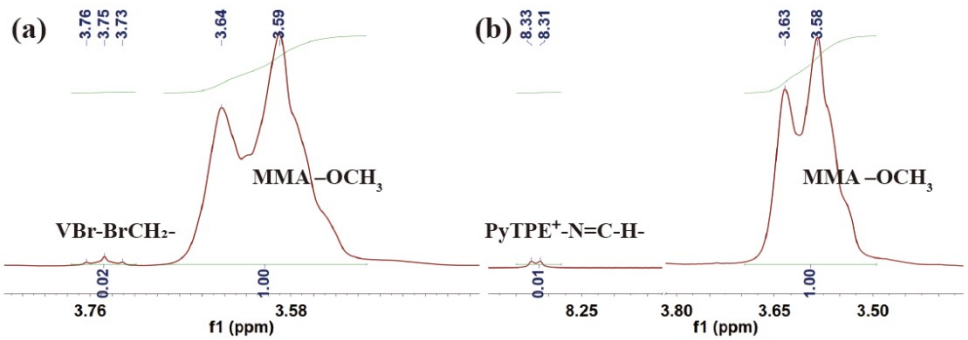

Figure S15. Changes of ^{1}H NMR characteristic peaks before and after Pyridyl-bromo alkylation reaction. (a) ^{1}H NMR of PBMB; (b) ^{1}H NMR of PBMB-PyTPE. The solvent was $CDCl_3$ (δ (^{1}H) = 7.26 ppm).

Comments: Functionalized molar ratio was determined by measuring the resonance intensities of PyTPE$^+$-N=C-H- and VBr-BrCH_2- at 8.33 and 3.73 ppm respectively, and the resonance intensities of MMA –OCH_3 3.62 ppm was used as the internal standard as shown in Fig. S15. The pyridine-functionalized molar ratio = $\frac{\int 8.33ppm/2}{\int 3.62ppm/2} : \frac{\int 3.73ppm/2}{\int 3.62ppm/2} * 100\% = 50\%$

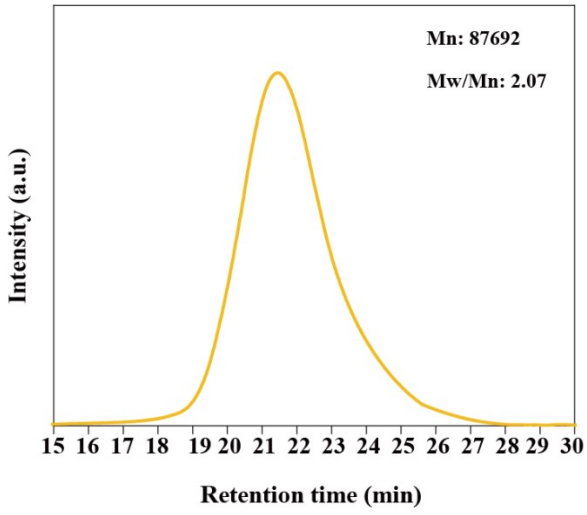

Figure S16. Size exclusion chromatogram for PBMB. SEC condition: eluent = THF, temperature = R.T. As shown, the Mn and PDI are 87692 g*mol^{-1} and 2.07, respectively.

Table S1. Characterization of PBMB.

	Feed molar ratio BA:MMA:VBr	Actual molar ratio* BA: MMA: VBr	Functionalized molar ratio** PyTPE : VBr	Mn*** g/mol	PDI***
PBMB	60:40:3	46:52:1.57	1:2	87692	2.07

* See details in Fig. S3.

** See details in Fig. S15.

*** Mn and PDI for PBMB were tested by GPC (see details in section 2.5), and the size exclusion

chromatogram was shown in Fig. S16.

Table S2. Crack width measured by AI measurement tool at selected points after different healing time at R.T. and 40°C.

	Time	Point 1	Point 2	Point 3	Average (μm) *	η_{PLM}
R.T.	0h	0.8554	0.6572	0.5561	5.30436	0
	1h	0.6202	0.4179	0.3236	3.49154	34%
	2h	0.5359	0.2292	0.2056	2.48897	53%
	3h	0.321	0.2696	0.1239	1.83205	65%
	4h	0.1163	0.0834	0.0723	0.69744	86%
40°C	0h	2.993	2.7234	2.8042	8.87562	0
	0.5h	1.5369	2.5346	1.6718	5.9826	33%
	1h	0.0809	0.3775	0.0404	0.51958	94%

*Average (R.T.) =Ave (point 1 + point 2 + point 3)/13*100 μm

Average (40 °C) =Ave (point 1 + point 2 + point 3)/16*50 μm

Where 13(16) and 100(50)μm were the lengths of scale bar in photos and in actual, respectively.

Table S3. Fluorescence intensity read by MATLAB data cursor tool at selected points after different healing time at R.T.*

	Point 1	Point 2	Point 3	Point 4	Point 5	Average	η_{CLSM}
0h	55	39	33	48	89	52.8	0%
1h	93	135	58	96	101	96.6	20%
2h	191	231	171	71	211	175	56%
3h	191	231	171	71	211	203.8	69%
4h	218	255	250	145	230	219.6	76%

*Original fluorescence intensity value calculated by the mean of fifteen-points, equaled to 255.

REFERENCE

1. Y. Liu, S. Chen, J. W. Y. Lam, P. Lu, R. T. K. Kwok, F. Mahtab, H. S. Kwok and B. Z. Tang, *Chemistry of Materials*, 2011, **23**, 2536-2544.
2. J. Xu, Y. Zhang, H. Zhou, Y. Hong, B. Zuo, X. Wang and L. Zhang, *Macromolecules*, 2017, **50**, 5905-5913.
3. B. Sun, Y. Lin, P. Wu and H. W. Siesler, *Macromolecules*, 2008, **41**, 1512-1520.
4. M. W. Urban, D. Davydovich, Y. Yang, T. Demir, Y. Zhang and L. Casabianca, *Science*, 2018, **362**, 220.
5. J. Huang, L. Zhang, Z. Tang, S. Wu and B. Guo, *Composites Science and Technology*, 2018, **168**, 320-326.
6. D. A. Long, *Journal of Raman Spectroscopy*, 2004, **35**, 905-905.
7. L. Zhang, H. Wang, Y. Zhu, H. Xiong, Q. Wu, S. Gu, X. Liu, G. Huang and J. Wu, *ACS Applied Materials & Interfaces*, 2020, **12**, 53239-53246.
8. H. Xiong, L. Zhang, Q. Wu, H. Zhang, Y. Peng, L. Zhao, G. Huang and J. Wu, *Journal of Materials Chemistry A*, 2020, **8**, 24645-24654.
9. H. Kitao, A. Takada and N. Nemoto, *Nihon Reoroji Gakkaishi(Journal of the Society of Rheology, Japan)*, 1997, **25**, 201-202.

10. N. K. Tierney and R. A. Register, *Macromolecules*, 2002, **35**, 6284-6290.
11. S. Atiqur Rahman, H. Kitao and N. Nemoto, *Polymer*, 2004, **45**, 4523-4532.
12. A. Takada, *Theoretical and Applied Mechanics Japan*, 2005, **54**, 255-261.
13. Y. Gao, N. R. Choudhury and N. K. Dutta, *Journal of Applied Polymer Science*, 2012, **126**, E130-E141.
14. J. Greener, J. R. Gillmor and R. C. Daly, *Macromolecules*, 1993, **26**, 6416-6424.
15. D. Basu, A. Das, K. W. Stöckelhuber, D. Jehnichen, P. Formanek, E. Sarlin, J. Vuorinen and G. Heinrich, *Macromolecules*, 2014, **47**, 3436-3450.
16. M. Lipińska, M. Gaca and M. Zaborski, *Polymer Bulletin*, 2021, **78**, 3199-3226.
17. R. A. Weiss, J. J. Fitzgerald and D. Kim, *Macromolecules*, 1991, **24**, 1071-1076.
18. N. K. Tierney and R. A. Register, *Macromolecules*, 2002, **35**, 2358-2364.
19. R. A. Weiss and H. Zhao, *Journal of Rheology*, 2008, **53**, 191-213.
20. W. Wang, J. Madsen, N. Genina, O. Hassager, A. L. Skov and Q. Huang, *Macromolecules*, 2021, **54**, 2306-2315.
21. U. H. Choi, Y. Ye, D. Salas de la Cruz, W. Liu, K. I. Winey, Y. A. Elabd, J. Runt and R. H. Colby, *Macromolecules*, 2014, **47**, 777-790.
22. X. Cao, X. Yu, J. Qin and Q. Chen, *Macromolecules*, 2019, **52**, 8771-8780.
23. M. T. Gabr and F. C. Pigge, *RSC Advances*, 2015, **5**, 90226-90234.
24. R. Chen, X. Gao, X. Cheng, A. Qin, J. Z. Sun and B. Z. Tang, *Polymer Chemistry*, 2017, **8**, 6277-6282.